IOPscience iopscience.iop.org

Home Search Collections Journals About Contact us My IOPscience

Spin waves in a doped antiferromagnet

This article has been downloaded from IOPscience. Please scroll down to see the full text article.

1991 J. Phys.: Condens. Matter 3 3537

(http://iopscience.iop.org/0953-8984/3/20/015)

View the table of contents for this issue, or go to the journal homepage for more

Download details:
IP Address: 171.66.16.147
The article was downloaded on 11/05/2010 at 12:07

Please note that terms and conditions apply.

J. Phys.: Condens. Matter 3 (1991) 3537–3550. Printed in the UK

Spin waves in a doped antiferromagnet

Junwu Gan, Natan Andrei and Piers Coleman
Physics Department, Rutgers University, Piscataway, NJ 08855, USA

Received 3 January 1991

Abstract. We have studied the doped antiferromagnet using a generalized t–J model which permits a semi-classical expansion about a magnetically ordered ground state. Of particular interest is the interplay between the spin backflow associated with holes and the coherent spin flow of the ordered magnet. A calculation of the leading-order spin-wave spectrum reveals a strong damping effect of the paramagnetic spin currents which, for small doping, renormalizes long-wavelength spin waves and causes short-wavelength spin waves to decay into particle–hole pair excitations. A correct Goldstone mode structure for the spin-wave spectrum is obtained only when the spin backflow is properly taken into account.

1. Introduction

The advent of heavy fermion and perovskite superconductivity has exposed major limitations in our understanding of the spin and charge dynamics close to an antiferromagnetic instability [1]. In more traditional magnetic conductors, magnetism appears as a spin polarization phenomenon. The coexistence of local moment behaviour with itineracy in the perovskite and heavy fermion superconductors, raises many new questions concerning the interplay between paramagnetic and magnetic degrees of freedom.

One of the more active areas of recent theoretical work concerns the nature of the magnetic order close to the metal–insulator transition. Work in this direction has been motivated by the perovskite superconductors, notably doped lanthanum cuprate, where long-range magnetism is absent, but short-range incommensurate correlation has been observed [2, 3]. One of the central issues in a discussion of doped antiferromagnets concerns how, if at all, the doping modifies the spin correlations. The one-band Hubbard model, and its close cousin, the 't–J' model are widely thought to provide an adequate framework for the discussion of the spin and charge dynamics in these systems. From a Hartree–Fock treatment of the Hubbard model, it has been known that the introduction of charge carriers tends to induce incommensurate order [4, 5]. In an incommensurate structure, the electrons become mobile, and the reduction in their kinetic energy offsets the increase in exchange energy associated with the distortion of the magnetic order. Within the Hartree–Fock theory, valid for small U, doping induces an incommensurate spin density wave. On the other hand, for large U, repulsive interactions between electrons severely suppress moment amplitude fluctuations, favoring transverse distortions of the antiferromagnetic order upon doping. Schraiman and Siggia [6] have suggested that a more likely result of

0953-8984/91/203537+14$03.50 © 1991 IOP Publishing Ltd

doping in a strongly interacting Mott insulators is the formation of an incommensurate helimagnet. The original Schraiman–Siggia approach adopted a long-wavelength, semi-classical model for the charge and spin degrees of freedom, and used an essentially static picture for the ordered state. Several more recent papers have developed the mean field picture of Schraiman and Siggia within the t–J model [7].

In this paper, we again return to this issue, using the Schraiman–Siggia hypothesis as a starting point to examine the effects of doping on spin dynamics. We are particularly interested in damping effects of charge motion on the spin degrees of freedom. This is a particularly important issue if we are to take steps towards an understanding of experimental neutron scattering results.

We shall limit our discussion within the confines of the t–J model

$$H = -\sum_{(i,j)} t_{ij}[\Psi^{+}_{i\sigma}\Psi_{j\sigma} + \mathrm{HC}] + J\sum_{\mathrm{NN}} \boldsymbol{S}_i \cdot \boldsymbol{S}_j . \tag{1}$$

For simplicity, the Heisenberg interaction is restricted to nearest neighbour (NN) sites, while the hopping term $t_{ij} = t$ and $t_{ij} = t'$ for nearest and next nearest neighbour sites respectively. These hopping terms in the t–J model generate the motion of holes in the magnetic background. As a hole moves, the strong constraint on the occupancy implies that the forward motion of charge is associated with a backflow of spin. The paramagnetic spin current along a given bond from site l to j can be written

$$\mathcal{J}^{p}_{l\to j} = -\mathrm{i}\, t_{lj}\, \Psi^{+}_{l\alpha}\left(\frac{\sigma_{\alpha\beta}}{2}\right)\Psi_{j\beta} + \mathrm{HC} \tag{2}$$

In the pure spin fluid, spin can also be transported in a coherent fashion via a distortion of the magnetic order. The 'magnetic component' of the spin current is given by

$$\mathcal{J}^{s}_{l\to j} = J_{lj}\boldsymbol{S}_l \times \boldsymbol{S}_j . \tag{3}$$

The total spin current is the sum of these two components which determines the equation of motion for the spins

$$\partial_t \boldsymbol{S}_i + \sum_j \mathcal{J}_{i\to j} = 0 \tag{4}$$

$$\mathcal{J}_{i\to j} = \mathcal{J}^{p}_{i\to j} + \mathcal{J}^{s}_{i\to j} . \tag{5}$$

In an ordered spiral magnet, the spin current along specific bonds acquires an expectation value due to the twist. Equilibrium occurs when the net uniform current vanishes. In a frustrated magnet, this cancellation occurs by a balance of the spin currents between nearest neighbour bonds, and further neighbour frustrating bonds. In a doped t–J model, the equilibrium of a twisted structure requires a cancellation between paramagnetic and 'magnetic' components of the current. At a mean field level, doping can be crudely considered as equivalent to static frustration [8], but clearly, the nature of this cancellation is quite different in the two cases, and deserves much closer examination.

In our analysis, we find that paramagnetic spin currents have a critical effect on transverse spin-wave modes. A spin wave can be regarded as a normal mode of spin current oscillations. Coupling between paramagnetic and magnetic spin currents induces damping and it must be included to conserve the total spin. If this damping is ignored, certain transverse Goldstone modes are artificially eliminated. Previous mean field treatments [7] resulted in two Goldstone modes at $\pm\boldsymbol{Q}/2$ for the spin-wave spectrum in a helimagnet with twisting wavevector $\boldsymbol{Q}$. General symmetry considerations actually imply that in a helimagnet, which is non-collinear, the correct spin-wave spectrum has three transverse Goldstone modes located at 0, $\pm\boldsymbol{Q}$ [9]. In our results we find that the inclusion of the dynamic effects of the damping restores the missing modes to the spectrum. In other words, static frustration effects of the holes are not sufficient to produce a spin conserving treatment of the doped Mott insulator.

Unlike its close cousin the Hubbard model, the t–J model suffers from a tendency to phase separation [10]. At low doping in this model, there is an effective attraction $V \sim t^2/J$ between holes that gives rise to unstable long-wavelength density fluctuation modes. From a purist's point of view, this pathology suggests that the t–J model does not provide an entirely faithful representation of the low-energy charge degrees of freedom in a large-U Hubbard model. A pragmatic way to evade this difficulty is to note that in practice, Coulomb interactions will always absorb these unstable modes into the plasma mode. In an array of conducting planes, each described by the t–J model, separated by a distance l and interacting purely through the Coulomb interaction, at low hole densities, the dielectric function has the form

$$\epsilon(\boldsymbol{q},\omega) \sim 1 - \left[\frac{4\pi e^2}{q^2} - Va^2 l\right]\chi_c(\boldsymbol{q},\omega) \tag{6}$$

where $\chi_c(\boldsymbol{q},\omega)$ is the dynamical charge susceptibility and a is separation of nearest neighbours in the plane. In the high-frequency, long-wavelength approximation $\chi_c \sim [q\omega_p(\boldsymbol{q})/e\omega]^2/4\pi$, where $\omega_p(\boldsymbol{q}) \sim 2\pi e^2\rho\sqrt{q}/m^*$ is the (two-dimensional) plasma frequency and ρ is the hole density, so zeros of the dielectric function then occur at

$$\omega_{\boldsymbol{q}}^2 = \omega_p^2(\boldsymbol{q})[1-(qa)^2(V/V_c)] \qquad (V_c = 4\pi e^2/l) \tag{7}$$

indicating that the long-wavelength phase separation instability is absorbed into the plasma mode. Provided that t/J is not too large, the possibility of short-wavelength instabilities can also be ignored.

In the work that follows, we develop a semi-classical treatment of the t–J model in the spirit of the large-S approach to quantum antiferromagnetism. A Schwinger boson representation is used for the spins, and the constrained electron creation operator is written as a product of a spin boson and a hole fermion[7]: $\Psi_{i\sigma}^{+} = b_{i\sigma}^{+} f_i$, where $b_{i\sigma}$ and f_i are Bose and Fermi operators respectively [11]. To control the fluctuations associated with the hole degrees of freedom, we introduce a fictitious conserved quantum number $\lambda = 1, \ldots, N$ to the hole operators $f_{i\lambda}$. The kinetic term in the Hamiltonian is now written

$$H = -\sum_{(i,j),\sigma\lambda} t_{ij}[\Psi_{i\lambda\sigma}^{+}\Psi_{j\lambda\sigma} + \mathrm{HC}] \tag{8}$$

where

$$\Psi_{i\lambda\sigma}^{+} = b_{i\sigma}^{+} f_{i\lambda} \qquad (\lambda = 1, \ldots, N)\,.$$

The constraint associated with the more general model is then

$$\sum_{\sigma} b_{i,\sigma}^{+} b_{i\sigma} + \sum_{\lambda} f_{i\lambda}^{+} f_{i\lambda} = 2S\,. \tag{9}$$

To develop a consistent large-S limit, we permit both N and S to grow, preserving the ratio $\gamma = N/2S$. In this way, both the kinetic and spin terms in the Hamiltonian scale extensively, as $O(\gamma S^2)$ and $O(S^2)$ respectively and the fluctuations in the spin and bilinear fermion operators are simultaneously quenched as $S \to \infty$. Our strategy is to evaluate the properties of the model in a $1/S$ expansion about this limit, ultimately returning to the t–J model by setting $\gamma = 1$ and $S = 1/2$.

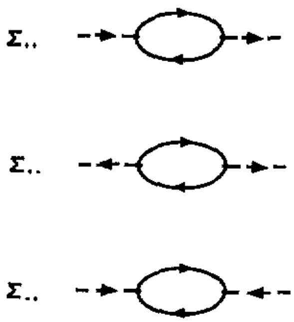

Figure 1. Spin-wave self-energy of $O(S)$ from particle–hole pair renomalization.

Perhaps the most surprising feature to emerge from this approach is the appearance of strong spin-charge coupling in the leading-order fluctuations. The effect of spin backflow on the spin-wave modes must be included on general symmetry grounds. Indeed, the spin-flip scattering of holes appears in the leading-order spin fluctuations (figure 1). We find that this induces strong spin-wave damping in the large-S limit which can cause destruction of long-range order for spin $S = 1/2$.

The organization of the paper is following. In the second section we present general symmetry considerations concerning the qualitative shape of spin excitation spectrum, as in the case of frustrated Heisenberg model. In the third section, we carry out semi-classical analysis to leading order consistently. We compute the spin wave spectrum and demonstrate explicitly the presence of three Goldstone modes at $\mathbf{0}, \pm\boldsymbol{Q}$. Finally, we discuss the properties of holes in this background, and the effect of higher-order terms in our expansion.

2. General symmetry considerations

In the $S \to \infty$ limit that we shall develop, the behaviour of our generalized t–J model (1) is determined by a saddle point, where, as we shall see, the spins develop long-range helimagnetic order with incommensurate magnetic wavevector $\boldsymbol{Q} = (Q_x, Q_y)$. In such a state, the local magnetization takes the form

$$\langle \boldsymbol{S}(\boldsymbol{R}) \rangle = 2S_{\boldsymbol{Q}}[\hat{\boldsymbol{u}} \cos \boldsymbol{Q} \cdot \boldsymbol{R} + \hat{\boldsymbol{v}} \sin \boldsymbol{Q} \cdot \boldsymbol{R}]$$

where $\hat{\boldsymbol{u}}$ and $\hat{\boldsymbol{v}}$ are orthogonal unit vectors. Quite generally, symmetry considerations determine the form of the low energy transverse spin-wave spectrum in such ordered antiferromagnetic structure. In any approximate treatment of the spin spectrum, consistency with these general considerations provides a check of whether the approach is spin conserving. In the case of helimagnetic structure with Heisenberg symmetry, invariance of the Hamiltonian with respect to uniform spin rotations leads to Goldstone modes at $\mathbf{0}$ and $\pm\mathbf{Q}$, corresponding to rotations about axes lying normal, and parallel to the spin plane. Rastelli [12] has applied these arguments to the frustrated Heisenberg model. The extension to the t–J model is strightforward, as we now show, following the formalism of Forster and Wagner[13, 14].

Let us examine the spin fluctuations normal to the plane of the precessing magnetization. Let $\hat{\boldsymbol{y}} = \hat{\boldsymbol{u}}$ and $\hat{\boldsymbol{z}} = \hat{\boldsymbol{v}}$ define the co-ordinate axes in spin plane, then the spectral function for spin fluctuations normal to the spin plane is

$$\chi''(\omega, \boldsymbol{q}) = \int_{-\infty}^{+\infty} \mathrm{d}t \, \langle [S^x_{\boldsymbol{q}}(t), S^x_{-\boldsymbol{q}}(0)] \rangle \mathrm{e}^{\mathrm{i}\omega t} \, . \tag{10}$$

The corresponding static susceptibility $\chi(\boldsymbol{q})$ and the density of states $\rho(\boldsymbol{q},\omega)$, with energy $\omega > 0$ and momentum $\boldsymbol{q}$, that are excited by $S^x_{-\boldsymbol{q}}$ are then

$$\chi(\boldsymbol{q}) = \mathcal{P} \int_{-\infty}^{+\infty} \frac{\mathrm{d}\omega}{2\pi} \frac{\chi''(\boldsymbol{q},\omega)}{\omega} \tag{11}$$

$$\rho(\boldsymbol{q},\omega) = \frac{1}{\omega\chi(\boldsymbol{q})} \chi''(\boldsymbol{q},\omega) \qquad \omega > 0 \qquad \beta\omega \ll 1 \, . \tag{12}$$

where $\mathcal{P}$ denotes the principle part. From (11) and (12), the second moment of the spectral density for the operator $S^x_{-\boldsymbol{q}}$ is

$$\overline{\omega^2_{\boldsymbol{q}}} = \int_{-\infty}^{+\infty} \frac{\mathrm{d}\omega}{2\pi} \, \rho(\boldsymbol{q},\omega)\omega^2 = \chi(\boldsymbol{q})^{-1} \int_{-\infty}^{+\infty} \frac{\mathrm{d}\omega}{2\pi} \, \omega \, \chi''(\boldsymbol{q},\omega) \, . \tag{13}$$

For small q, spin conservation implies that the numerator in this expression is proportional to q^2, so $\overline{\omega^2_{\boldsymbol{q}}} \to 0$, as $\boldsymbol{q} \to 0$, since the static susceptibility $\chi(\boldsymbol{q})$ is finite in this limit. To see this, we write

$$\int_{-\infty}^{+\infty} \frac{\mathrm{d}\omega}{2\pi} \, \omega \, \chi''(\boldsymbol{q},\omega) = \left\langle [[S^x_{\boldsymbol{q}} \, , H], S^x_{-\boldsymbol{q}}] \right\rangle . \tag{14}$$

Spin conservation forces the commutator to vanish at $q = 0$, and inversion symmetry implies that the whole expression must vanish at least as fast as q^2.

For $\boldsymbol{q} \to \pm\boldsymbol{Q}$, the numerator of (13) tends to a constant, while the slow transverse fluctuations in the magnetization induce a divergence of the staggered transverse susceptibility $\chi(\boldsymbol{q})$, which in turn leads to $\overline{\omega^2_{\boldsymbol{q}}}$ vanishing as $(\boldsymbol{q} \pm \boldsymbol{Q})^2$. On general hydrodynamic grounds, the long-wavelength static fluctuations of the spins behave classically, and the long-wavelength fluctuations are given by the inverse of the classical action. The fluctuations in the vicinity of $\boldsymbol{q} \sim \pm\boldsymbol{Q}$ are

$$\chi(\boldsymbol{q}) \simeq \frac{S^2_{\boldsymbol{Q}}}{(\delta\boldsymbol{q} \cdot \mathcal{R}_{\mathrm{s}} \cdot \delta\boldsymbol{q})} \qquad \delta\boldsymbol{q} = \boldsymbol{q} \pm \boldsymbol{Q} \tag{15}$$

where $\mathcal{R}_{\mathrm{s}}$ is the spin-wave stiffness tensor. One can place an upper bound on the spin-wave stiffnesses by using Bogoliubov inequality ($\chi_{A^\bullet \, A} \, \chi_{B^\bullet \, B} \geq |\chi_{A^\bullet \, B}|^2$)

$$\chi(\boldsymbol{q}) \geq \frac{|\langle [S^y_{\boldsymbol{q}\pm\boldsymbol{Q}} \, , S^x_{-\boldsymbol{q}}] \rangle|^2}{\left\langle [[S^y_{\boldsymbol{q}\pm\boldsymbol{Q}} \, , H], S^y_{-\boldsymbol{q}\mp\boldsymbol{Q}}] \right\rangle} . \tag{16}$$

The commutator in the numerator is

$$\langle [S^y_{q\pm Q}, S^x_{-q}] \rangle = -\mathrm{i}\, S^z_{\pm Q} \,. \tag{17}$$

and for the spiral order assumed above $|\langle S^z_{\pm Q} \rangle| = S_Q$ which is just the spiral magnetization, so the denominator provides an upper bound on the eigenvalues of the spinwave stiffness tensor. The action of the spin operators within the commutator in the denominator is to 'twist' the Hamiltonian. Evaluating this commutator for the t–J model we find

$$[[S^y_q, H], S^y_{-q}] = \mathcal{N}^{-1}[H^y(q) - H^y(0)] \tag{18}$$

where $\mathcal{N}$ is the number of lattice sites and

$$H^y(q) = -\frac{1}{2}\sum_{(i,j)} t_{ij}\Psi^\dagger_{i\sigma}\Psi_{j\sigma}\cos(q\cdot R_{ij}) + \mathrm{HC} + 2J\sum_{\mathrm{NN}}(S_i\cdot S_j - S^y_i S^y_j)\cos(q\cdot R_{ij}) \tag{19}$$

with $R_{ij} = R_i - R_j$. Expanding about $q = 0$ we obtain an upper bound on the stiffness given by

$$[\mathcal{R}_s]^{\alpha\beta} = \frac{1}{2\mathcal{N}}\sum_{(i,j)} t_{ij}(R_{ij})^\alpha (R_{ij})^\beta \langle \Psi^+_{i\sigma}\Psi_{j\sigma}\rangle + \frac{J}{\mathcal{N}}\sum_{\mathrm{NN}}(R_{ij})^\alpha(R_{ij})^\beta(\langle S^y_i S^y_j\rangle - \langle S_i S_j\rangle)\,. \tag{20}$$

In practice, spin current fluctuations will always reduce the stiffness below this upper bound [9].

Note finally, that we can combine the results of this section into a compact upper bound for the entire transverse spin-wave spectrum

$$\overline{\omega_q}^2 \le \overline{\omega_q^2} \le S_Q^{-2}[E^x(q) - E^x(0)]\,[E^y(q\pm Q) - E^y(0)] \tag{21}$$

where

$$E^\alpha(q) = \mathcal{N}^{-1}\langle H^\alpha(q)\rangle\,. \tag{22}$$

This upper bound can be used as a single mode approximation to the transverse spin-wave spectrum.

3. Renormalized spin wave

In this section, we shall use $1/S$ as the small parameter to do a combined large-S and large-N expansion with ratio $N/2S$ fixed. To leading order, the fermion spectrum is not modified. However, the spin wave spectrum is strongly renormalized by particle–hole excitations. We shall calculate the renormalized spin-wave spectrum and show explicitly how the correct Goldstone mode structure is restored by particle–hole renormalization in our systematic expansion. Near Goldstone modes, the spin-wave spectrum is linear. We shall calculate the renormalized spin-wave velocity in the small doping limit which becomes, in this case, anisotropic due to coupling with particle-hole excitations. In the next section, we shall discuss what is probable modification of the leading-order picture, when we take into consideration higher-order contributions, which will give us insights for the spin $S = 1/2$ problem.

We first rotate independently the spin basis at each site such that the new reference frame is locally ferromagnetic[9]. The Hamiltonian in the new reference frame is

$$H = -\sum_{(i,j)} t_{ij} f_{i\lambda} f_{j\lambda}^{+} b_i^{+} \exp(\tfrac{1}{2}\mathrm{i}\theta_{ij}\, \boldsymbol{n}_{ij}\cdot\boldsymbol{\sigma}) b_j + \mathrm{HC} + J\sum_{\mathrm{NN}} \sin\theta_{ij}\, \boldsymbol{n}_{ij}\cdot(\boldsymbol{S}_i\times\boldsymbol{S}_j)$$
$$+ J\sum_{\mathrm{NN}} \{(\boldsymbol{S}_i\cdot\boldsymbol{n}_{ij})(\boldsymbol{S}_j\cdot\boldsymbol{n}_{ij}) + \cos\theta_{ij}[\boldsymbol{S}_i\cdot\boldsymbol{S}_j - (\boldsymbol{S}_i\cdot\boldsymbol{n}_{ij})(\boldsymbol{S}_j\cdot\boldsymbol{n}_{ij})]\} \quad (23)$$

where $b^{+} = (b_{\uparrow}^{+}, b_{\downarrow}^{+})$, the unit vector $\boldsymbol{n}_{ij}$ is the axis required to rotate coordinate system at site j into coordinate system i, and θ_{ij} is the angle of rotations between two local reference frames.

In the $S \to \infty$ case, the ground state reduces to the classical configuration. We look for a simple twist solution: $\boldsymbol{n}_{ij}$ =constant, $\theta_{ij} = \boldsymbol{Q}\cdot\boldsymbol{R}_{ij}$ with twisting wavevector $\boldsymbol{Q} = (Q_x, Q_y)$.

$$\frac{H}{\mathcal{N}} \overset{S\to\infty}{=} (2S)^2(1-\rho\gamma)E_0 \quad (24)$$

$$E_0 = 2\gamma\sum_{\boldsymbol{\delta}} t_{\boldsymbol{\delta}}\, g_{\boldsymbol{\delta}} \cos\frac{Q_{\boldsymbol{\delta}}}{2} + \frac{1-\rho\gamma}{4}\sum_{\boldsymbol{\delta}} J_{\boldsymbol{\delta}} \cos Q_{\boldsymbol{\delta}} \quad (25)$$

where $\boldsymbol{\delta}$ summation runs over nearest and next nearest neighbour vectors and $Q_{\boldsymbol{\delta}} = \boldsymbol{Q}\cdot\boldsymbol{\delta}$. We set the lattice constant equal to one for convenience. $J_{\boldsymbol{\delta}} \neq 0$ only for nearest neighbour vectors $\boldsymbol{\delta}$. We use $g_{\boldsymbol{\delta}}$ to denote the averaged hopping amplitude

$$g_{\boldsymbol{\delta}} = \langle f_{i\lambda}^{+} f_{j\lambda}\rangle \qquad \boldsymbol{\delta} = \boldsymbol{R}_i - \boldsymbol{R}_j \quad (26)$$

where we do *not* sum over λ. The four neighbouring hopping amplitudes will be explicitly denoted as g_x, g_y, g_+, g_- for $\boldsymbol{\delta} = \boldsymbol{x}, \boldsymbol{y}, \boldsymbol{x}+\boldsymbol{y}, \boldsymbol{x}-\boldsymbol{y}$, respectively. The other parameters are $\gamma = N/2S$ and the doping $\rho = \langle f_{i\lambda}^{+} f_{i\lambda}\rangle$, i.e. fermion density per flavour. The twisting wavevector is obtained by minimizing equation (25): $\partial_{\boldsymbol{Q}} E_0 = 0$. For small t', the vector $\boldsymbol{Q}$ is diagonal: $Q_x = Q_y = Q$, $g_x = g_y = g$. Then, we obtain explicitly

$$\cos\left(\frac{Q}{2}\right) = -\frac{2gt\gamma}{J(1-\rho\gamma) + 4g_{+}t'\gamma}. \quad (27)$$

Fluctuations about the classical configuration are spin waves. To explore the spin-wave properties, we use the usual Holstein–Primakoff expansion. We choose the twisting axis to be the x axis: $\boldsymbol{n}_{ij} = \boldsymbol{x}$. Then

$$b_{i\uparrow} = b_{i\uparrow}^{+} = \left(2S - \sum_{\lambda} f_{i\lambda}^{+} f_{i\lambda} - b_i^{+} b_i\right)^{1/2}$$
$$b_{i\downarrow} = b_i \quad (28)$$
$$b_{i\downarrow}^{+} = b_i^{+}\,.$$

Here, b_i and b_i^+ are Holstein-Primakoff Bose operators. After expanding Hamiltonian (23) in the large S limit and keeping the relevant terms for our purpose, we find

$$\begin{aligned}
H &= H_{cl} + H_0 + H_1 \\
H_{cl} &= \mathcal{N} J \tilde{S}^2 (\cos Q_x + \cos Q_y) + \sum_{k} \varepsilon(k) f^+_{k,\lambda} f_{k,\lambda} \\
H_0 &= \sum_q \left(h_q b^+_q b_q + \frac{\Delta_q}{2} (b_q b_{-q} + \mathrm{HC}) \right) \\
H_1 &= \sqrt{\frac{1}{\mathcal{N}}} \sum_{k,q} f^+_{k+q/2,\lambda} f_{k-q/2,\lambda} u(k,q) b_q + \mathrm{HC}
\end{aligned} \tag{29}$$

where we have introduced the following short-hand notation:

$$\begin{aligned}
\varepsilon(k) &= 4\tilde{S} \sum_\delta t_\delta \cos\left(\frac{Q_\delta}{2}\right) \cos k_\delta - \mu \\
h_q &= \sum_\delta \left[4S\gamma t_\delta g_\delta \cos\left(\frac{Q_\delta}{2}\right)(\cos q_\delta - 1) + \tilde{S} J_\delta [(1+\cos Q_\delta)\cos q_\delta - 2\cos Q_\delta] \right] \\
\Delta_q &= \tilde{S} \sum_\delta J_\delta (1 - \cos Q_\delta) \cos q_\delta \\
u(k,q) &= \sqrt{2\tilde{S}} \sum_\delta \left[-2t_\delta \sin\left(\frac{Q_\delta}{2}\right) \cos\left(\frac{q_\delta}{2}\right) \sin k_\delta + 2t_\delta \sin\left(\frac{Q_\delta}{2}\right) \sin\left(\frac{q_\delta}{2}\right) \cos k_\delta \right. \\
&\quad \left. - \frac{1}{2} J_\delta \sin Q_\delta \sin q_\delta - \frac{\gamma}{\sqrt{1-\rho\gamma}} t_\delta g_\delta \sin\left(\frac{Q_\delta}{2}\right) \sin q_\delta \right].
\end{aligned} \tag{30}$$

Here $\tilde{S} = S(1-\rho\gamma)$ is the reduced spin magnitude. In the Fermionic spectrum, μ is the chemical potential which is determined by doping.

The resulting Hamiltonian (29) describes a system of spin fluctuations coupled to fermions. The coupling arises from the association of the spin backflow with forward charge current. We note that the interacting vertex coupling constant $u(k,q)$ is $O(\sqrt{S})$. Since both the bare fermionic and bosonic propagators are of order $1/S$, a perturbative treatment in $1/S$ is suitable in the large-S limit. To leading order, we see that spin fluctuations have no effect on fermion dynamics. The fermionic propagator is simply the free one

$$\xrightarrow{k,\,\mathrm{i}\omega_n} = G_{\lambda\lambda'}(k, \mathrm{i}\omega_n) = G(k, \mathrm{i}\omega_n)\delta_{\lambda\lambda'} = \frac{\delta_{\lambda\lambda'}}{\mathrm{i}\omega_n - \varepsilon(k)}. \tag{31}$$

But the spin-wave spectrum is renormalized by the interactions due to the presence of N flavours of fermions. We can define the spin-wave propagator matrix as

$$\mathsf{D}(\mathrm{i}\nu_n, q) = \begin{pmatrix} \langle b^+_q(\mathrm{i}\nu_n)\, b_q(\mathrm{i}\nu_n)\rangle & \langle b^+_q(\mathrm{i}\nu_n)\, b^+_{-q}(-\mathrm{i}\nu_n)\rangle \\ \langle b_q(\mathrm{i}\nu_n)\, b_{-q}(-\mathrm{i}\nu_n)\rangle & \langle b_{-q}(-\mathrm{i}\nu_n)\, b^+_{-q}(-\mathrm{i}\nu_n)\rangle \end{pmatrix}. \tag{32}$$

The relevant contributions to the self-energy of the spin-wave propagator are three diagrams shown in figure 1. They can be compactly written as

$$\boldsymbol{\Sigma}(\mathrm{i}\nu_n, \boldsymbol{q}) = \begin{pmatrix} \Sigma_{++}(\mathrm{i}\nu_n, \boldsymbol{q}) & \Sigma_{+-}(\mathrm{i}\nu_n, \boldsymbol{q}) \\ \Sigma_{-+}(\mathrm{i}\nu_n, \boldsymbol{q}) & \Sigma_{++}(-\mathrm{i}\nu_n, -\boldsymbol{q}) \end{pmatrix} . \tag{33}$$

The full leading-order spin-wave propagator is

$$\mathsf{D}^{-1}(\mathrm{i}\nu_n, \boldsymbol{q}) = \begin{pmatrix} \mathrm{i}\nu_n - h_{\boldsymbol{q}} - \Sigma_{++}(\mathrm{i}\nu_n, \boldsymbol{q}) & -\Delta_{\boldsymbol{q}} - \Sigma_{+-}(\mathrm{i}\nu_n, \boldsymbol{q}) \\ -\Delta_{\boldsymbol{q}} - \Sigma_{-+}(\mathrm{i}\nu_n, \boldsymbol{q}) & -\mathrm{i}\nu_n - h_{\boldsymbol{q}} - \Sigma_{++}(-\mathrm{i}\nu_n, -\boldsymbol{q}) \end{pmatrix} . \tag{34}$$

The explicit expression for the spin-wave self-energy is

$$\Sigma_{\alpha\beta}(\mathrm{i}\nu_n, \boldsymbol{q}) = \frac{2S\gamma}{\mathcal{N}} \sum_{\boldsymbol{k}} \Pi(\boldsymbol{k}, \boldsymbol{q}, \mathrm{i}\nu_n) u(\boldsymbol{k}, \alpha\boldsymbol{q}) u(\boldsymbol{k}, \beta\boldsymbol{q}) \qquad \alpha, \beta = +, - . \tag{35}$$

In the last expression, we denote the fermionic polarization bubble in figure 1 by

$$\Pi(\boldsymbol{k}, \boldsymbol{q}, \mathrm{i}\nu_n) = \frac{f(\varepsilon_{\boldsymbol{k}-\boldsymbol{q}/2}) - f(\varepsilon_{\boldsymbol{k}+\boldsymbol{q}/2})}{\mathrm{i}\nu_n + \varepsilon(\boldsymbol{k} - \boldsymbol{q}/2) - \varepsilon(\boldsymbol{k} + \boldsymbol{q}/2)} \tag{36}$$

where $f(\varepsilon_{\boldsymbol{k}})$ is the Fermi–Dirac distribution function. Straightforward algebraic calculations lead to following implicit equation which determines the spin-wave spectrum $\omega = \omega(\boldsymbol{q})$:

$$\omega - A(\omega, \boldsymbol{q}) = \sqrt{[h_{\boldsymbol{q}} + S(\omega, \boldsymbol{q})]^2 - [\Delta_{\boldsymbol{q}} + \Sigma_{+-}(\omega, \boldsymbol{q})]^2} \tag{37}$$

where

$$\begin{aligned} S(\omega, \boldsymbol{q}) &= \tfrac{1}{2}[\Sigma_{++}(\omega, \boldsymbol{q}) + \Sigma_{++}(-\omega, -\boldsymbol{q})] \\ A(\omega, \boldsymbol{q}) &= \tfrac{1}{2}[\Sigma_{++}(\omega, \boldsymbol{q}) - \Sigma_{++}(-\omega, -\boldsymbol{q})] . \end{aligned} \tag{38}$$

If we do not include particle–hole contributions, that is, if we neglect the Boson self-energy $\Sigma_{\alpha\beta}(\mathrm{i}\nu_n, \boldsymbol{q})$, then it is easy to see that the spin-wave spectrum has Goldstone modes at $\boldsymbol{0}$, but not at $\pm\boldsymbol{Q}$, which violates the symmetry requirement. Including fermionic renormalization, which is consistent in the $1/S$ expansion, will restore the correct symmetry as discussed in the previous sections. Now, we can explicitly verify that $\boldsymbol{0}, \pm\boldsymbol{Q}$ are Goldstone modes. For instance, we can put $\omega(\boldsymbol{Q}) = 0$ into equation (37) to verify $A(0, \boldsymbol{Q}) = 0$ and $h_{\boldsymbol{Q}} + \Delta_{\boldsymbol{Q}} + S(0, \boldsymbol{Q}) + \Sigma_{+-}(0, \boldsymbol{Q}) = 0$. To show this, we note that $u(-\boldsymbol{k}, -\boldsymbol{q}) = -u(\boldsymbol{k}, \boldsymbol{q})$ and $\Pi(-\boldsymbol{k}, -\boldsymbol{q}, \mathrm{i}\nu_n) = \Pi(\boldsymbol{k}, \boldsymbol{q}, \mathrm{i}\nu_n)$, so we can rewrite

$$A(\omega, \boldsymbol{q}) = \frac{2S\gamma}{\mathcal{N}} \sum_{\boldsymbol{k}} [\Pi(\boldsymbol{k}, \boldsymbol{q}, \omega) - \Pi(\boldsymbol{k}, \boldsymbol{q}, -\omega)] u^2(\boldsymbol{k}, \boldsymbol{q}) .$$

We can also rewrite

$$S(\omega, \boldsymbol{q}) + \Sigma_{+-}(\omega, \boldsymbol{q}) = \frac{S\gamma}{\mathcal{N}} \sum_{\boldsymbol{k}} \Pi(\boldsymbol{k}, \boldsymbol{q}, \omega) [u(\boldsymbol{k}, \boldsymbol{q}) + u(\boldsymbol{k}, -\boldsymbol{q})]^2 .$$

So at $q = Q$, $\omega = 0$

$$S(0,Q) + \Sigma_{+-}(0,Q) = \frac{2S\gamma}{\mathcal{N}} \sum_{k} [f(\varepsilon_{k-Q/2}) - f(\varepsilon_{k+Q/2})] \sum_{\delta} t_\delta \sin Q_\delta \sin k_\delta$$

$$= \frac{4S\gamma}{\mathcal{N}} \sum_{\delta} t_\delta g_\delta \sin Q_\delta \sin\left(\frac{Q_\delta}{2}\right).$$

This exactly cancels $h_Q + \Delta_Q$ from (30). We note that, in contrast to the Heisenberg model, $\pm(Q_y, Q_x)$ are not zero modes, breaking the crystal point group symmetry in the large-S limit. This is because even in the large-S limit, surrounding spin condensate, there are always spin fluctuations coupled with charge fluctuations. These fluctuations violate the crystal point group symmetry[9]. It is interesting to note that the asymmetric part of the self-energy $A(\omega, q)$ does not vanish in this case, in contrast to the Bosonic exchange contributions resulting from three magnon interacting vertex in the pure frustrated Heisenberg model [12]. The difference comes from the fact that in pure Bose system the Bosons can only propagate forward, whereas in this case magnons are coupled with the Fermionic system in which there are both quasiparticle forward propagation and quasihole backward propagation.

The implicit spectrum equation (37) in the general case is difficult to solve. For $t' \ll t$, the twisting wavevector is diagonal, $Q = (Q, Q)$. We shall limit the following discussion to this case. In the particular case of t–J model, *i.e.* $t' = 0$, the spin excitations are highly degenerate along the line $q_x = q_y = q$ in the Brillouin zone in the large-S limit. This degeneracy is removed by the presence of the next nearest neighbour hopping t'. However, we think this degeneracy is unphysical when $t' = 0$. Once one continues to the small S, we do expect that this degeneracy is lifted by high order terms (see the discussion by Shraiman Siggia [6]).

For the long-wavelength spin waves near the Goldstone mode $\mathbf{0}$, we write $q = (1, \eta)q$, $q \to 0$, with the parameter η determining the direction of approaching the long-wavelength limit. We then carry out small q expansion

$$h_q + \Delta_q \simeq 4\tilde{S}J(1 - \cos Q) \tag{39}$$

$$h_q - \Delta_q \simeq 2S\xi\, q^2 \tag{40}$$

with

$$\xi = -\left[\frac{J}{2}(1 - \rho\gamma)\cos Q + gt\gamma \cos\left(\frac{Q}{2}\right)\right](1 + \eta^2) - t'\gamma\left[g_+ \cos Q(1 + \eta)^2 + g_-(1 - \eta)^2\right].$$

So, we obtain the equation which determines the renormalized spin-wave velocity $c = \omega/(q\sqrt{1 + \eta^2})$,

$$c\sqrt{1 + \eta^2} = A(c) + \sqrt{[2S\xi + Y_\varphi(c)][4\tilde{S}J(1 - \cos Q) + Y_\vartheta(c)]} \tag{41}$$

where

$$\begin{aligned} &A(\omega, q) \simeq A(c)q \\ &S(\omega, q) + \Sigma_{+-}(\omega, q) \simeq Y_\vartheta(c) \\ &S(\omega, q) - \Sigma_{+-}(\omega, q) \simeq Y_\varphi(c)q^2 . \end{aligned} \tag{42}$$

Since the spectrum equation (37) is symmetric under inversion $q \to -q$, we limit our consideration for $q > 0$ only. The spin-wave velocity depends on η, so it is anisotropic.

For small doping and small t', specifically, assuming $\rho \sim t'/J \ll 1$, and $t^2\rho\gamma/J > t'$, we can expand the spin-wave velocity in powers of doping ρ up to $O(\rho^2)$,

$$c = c_0 + c_1\rho + c_2\rho^2 . \tag{43}$$

After purely algebraic calculation, we obtain

$$c_0 = 2\sqrt{2}SJ \tag{44}$$

$$c_1 = -\frac{4\sqrt{2}St^2\gamma}{J}\,\frac{(1+\eta)^2}{1+\eta^2} - \sqrt{2}SJ\gamma \tag{45}$$

where c_0 is just the AF spin-wave velocity. We have also obtained c_2, but it is too lengthy to write it explicitly. The spin-wave velocity is suppressed by doping and it is most suppressed along the direction of pitch. Taking $\gamma = 1$, the semi-classical result (43) suggests the instability of long-range order for $t^2\rho \sim J^2$.

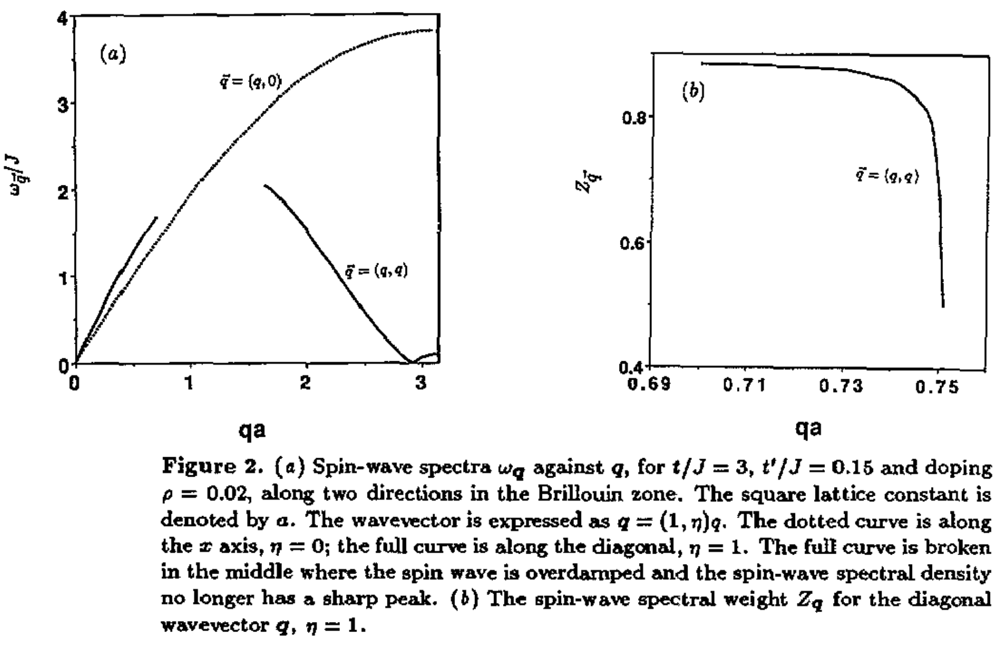

Figure 2. (a) Spin-wave spectra $\omega_{\boldsymbol{q}}$ against q, for $t/J = 3$, $t'/J = 0.15$ and doping $\rho = 0.02$, along two directions in the Brillouin zone. The square lattice constant is denoted by a. The wavevector is expressed as $\boldsymbol{q} = (1, \eta)q$. The dotted curve is along the x axis, $\eta = 0$; the full curve is along the diagonal, $\eta = 1$. The full curve is broken in the middle where the spin wave is overdamped and the spin-wave spectral density no longer has a sharp peak. (b) The spin-wave spectral weight $Z_{\boldsymbol{q}}$ for the diagonal wavevector $\boldsymbol{q}$, $\eta = 1$.

For arbitrary doping, the spectrum equation (37) has been solved numerically. The spectra for a particular set of parameter values are plotted in figure 2(a). Despite coupling with pair excitations, spin waves along the x direction and long-wavelength spin waves along the diagonal direction remain well defined to leading order. The reason is that decay of these spin waves into a single particle–hole pair is not possible in this case because the spin-wave velocity is larger than the Fermi velocity. We observe that along the diagonal direction of the Brillouin zone, some of the short-wavelength spin waves are overdamped due to decay into single particle–hole pair. This can be seen from figure 3, in which we plot the single particle–hole pair excitation continuum together with the spin-wave spectrum for the same parameter values of figure 2. Damping occurs in the region where spin-wave spectrum crosses the pair excitation

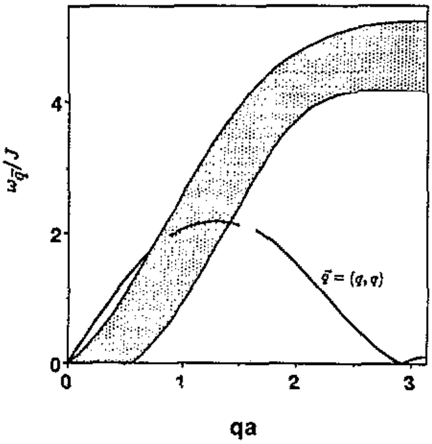

Figure 3. Spin-wave spectrum together with the continuum of particle–hole pair excitations (shaded area) for the same parameter values as in figure 2. The wavevector is along the diagonal direction, $\eta = 1$. The dotted curve in the damped spin-wave region is just a guide to the eye.

continuum. Damping is also manifested by the fact that the spin-wave spectral weight is increasingly transferred to particle–hole excitations as the wavelength decreases, before the real decay occurs. If we conveniently denote the spectrum equation (37) as $\omega - \Phi(\omega, \boldsymbol{q}) = 0$, then the spectral weight is defined as $Z_{\boldsymbol{q}} = [1 - \partial_\omega \Phi(\omega, \boldsymbol{q})]^{-1}_{\omega=\omega(\boldsymbol{q})}$. The spectral weight for $\boldsymbol{q}$ along the diagonal direction ($\eta = 1$) is plotted in figure 2(b). The spectral weight drops sharply to zero as the spectrum passes into pair excitation continuum and becomes overdamped.

As the doping increases above a certain threshold, $\rho > \rho_c$, the spin-wave spectrum is almost entirely dissolved in the pair excitations. In this case, even at long wavelengths, there are no sharp spin-wave excitations. Once $\rho > \rho_c$, the poles of the Green function given by (34) move off the real axis, acquiring a finite imaginary part: $\omega_{\boldsymbol{q}} - \mathrm{i}\,\Gamma_{\boldsymbol{q}}$. At long wavelength, $\Gamma_{\boldsymbol{q}}$ is linear in q. We plot the spectrum for the wavevector $\boldsymbol{q}$ along the diagonal direction ($\eta = 1$) in figure 4, for a set of particular values of physical parameters. In this case, even long-wavelength spin waves are overdamped.

The spin-wave damping is reminiscent of the Landau damping of coherent sound modes in the Fermi liquid (zero sound) [15]. When the sound velocity is larger than the Fermi velocity, the density modes can only decay into multiple particle–hole pairs; the resulting lifetime is long due to a small decay amplitude and little available phase space. Overdamping occurs when the density mode dissolves into pair excitation continuum, that is when the sound velocity is smaller than the Fermi velocity, so that it can decay into single particle–hole pair. The coherent density modes lose their identity. The origin of Landau damping is quasiparticle interaction; the spin-wave damping in our case is produced by the coupling of backflow spin currents to charge currents.

4. Discussion

We have shown in general the existence of three Goldstone modes in the spin-wave spectrum following the long-range spiral order hypothesis. The spectrum obtained in

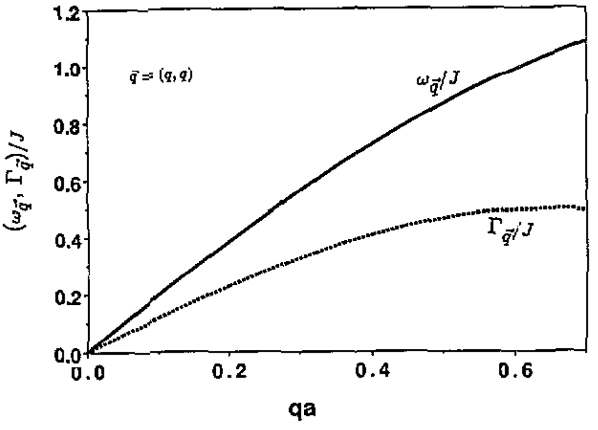

Figure 4. Damping of the long-wavelength spin waves for 5.2% doping. The parameter values are $t/J = 3$, $t'/J = 0.15$. The complex frequency $\omega_{\boldsymbol{q}} - \mathrm{i}\,\Gamma_{\boldsymbol{q}}$ is calculated for wavevector $\boldsymbol{q}$ along the diagonal direction ($\eta = 1$). The full curve is the real part of the frequency $\omega_{\boldsymbol{q}}$; the dotted one is damping coefficient $\Gamma_{\boldsymbol{q}}$.

our large-S expansion displays the correct Goldstone mode structure which can only be obtained in a spin-conserving treatment. This requires that one goes beyond the static frustration approximation and considers the coupling between spin and charge currents, underlying the strong correlation between hole motion and spin background. How does the leading-order picture, namely the conducting helimagnet, evolve when we continue to small spin S? To answer this question, we need to consider high order terms in the $1/S$ expansion.

To leading order spin waves are overdamped when they dissolve into pair excitation continuum. To second order, the holes can be scattered off spin fluctuations. Scattering by damped spin waves broadens the fermion quasiparticle excitations. Thus, we lose the well defined Fermi liquid limit even at $T = 0$. Long-wavelength spin waves can in turn be broadened by damped quasiparticle–quasihole pair excitations. However, for small doping $\rho < \rho_c$, only a small fraction of spin waves is damped and these damped spin waves have a quite high excitation energy; the resulting scattering amplitude is small. The corresponding lifetime for quasiparticles must, therefore, be quite long. We can view the system as being composed of long-wavelength spin excitations together with quasiparticles that weakly scatter each other. In this sense, we expect that the conducting helimagnet picture offered by the leading-order calculations is a good approximation, being essentially valid for the range of small frequencies but larger than the inverse of the lifetime.

When doping exceeds a certain threshold, the spin-wave spectrum is almost completely dissolved into the particle–hole pair excitation continuum. Even long wavelength spin waves can decay into particle–hole pairs. This means that most spin fluctuations are incoherent. Scattering of holes by these incoherent spin fluctuations significantly broadens the quasiparticle excitations. The presence of quite a large fraction of quantum spin fluctuations for the small-spin case, especially for $S = 1/2$, indicates that quasiparticles are damped rather rapidly. This means that the correlation between charge and spin excitations is so strong that it is improper to consider each of them separately. The nature of this state is unknown. Ramakrishnan [16] speculated that the long-range order cannot survive the strong decay of spin waves into particle–hole pair excitations, and the scattering of quasiparticles by spin excitations can lead to a linear frequency dependence for the imaginary part of quasiparticle self-energy. It is interesting to recall that the pair renormalization also leads to a finite lifetime for phonons in metals. Phonon spectrum certainly dissolves into the pair excitation continuum due to high electron density. But the imaginary part of the phonon self-energy is smaller than the real part of phonon frequency by a factor of (electron mass/ion mass).

There is some inconclusive evidence from neutron scattering experiments [2, 3], which points to the existence of an incommensurate spin correlation in doped La_2CuO_4. But, the correlation is only of short range and the correlation length is essentially temperature independent. According to our large-S calculation, spin waves are overdamped for just 5% doping for $t/J = 3$ figure 4. This can be regarded as the precursor of depleting long-range order for spin $S = 1/2$. Clearly, the actual spin dynamics is much more complicated than what the simple semi-classical picture can offer. It is not clear as to whether the topological effects play a significant role.

Acknowledgments

JG wants to thank F Mila for many discussions. Part of this work was supported by NSF grant DMR-89-13692. PC is a Sloan Foundation Fellow.

References

[1] Anderson P W 1988 50 years of the Mott phenomenon *Frontiers and Borderlines in Many-Particle Physics* (Corso: CIV)

[2] Shirane G, Birgeneau R J, Endoh Y, Gehring P, Kastner M A, Kitazawa K, Kojima H, Tanaka I, Thurton T R and Yamada K 1989 *Phys. Rev. Lett.* **63** 330
Thurston T R *et al* 1989 *Phys. Rev.* B **40** 4585

[3] Hayden S M, Aeppli G, Mook H, Rytz D, Hundley M F and Fisk Z 1991 *Phys. Rev. Lett.* **66** 821

[4] See for example Affleck's lecture notes for a simple discussion: Affleck I 1989 *1988 Les Houches, Session XLIX* ed E Brézin and J Zinn-Justin (Amsterdam: Elsevier)

[5] Schulz H J 1990 *Phys. Rev. Lett.* **64** 1445

[6] Shraiman B I and Siggia E D 1988 *Phys. Rev. Lett.* **61** 467; 1989 *Phys. Rev. Lett.* **62** 1564

[7] Jayaprakash C, Krishnamurthy H R and Sarkar S 1989 *Phys. Rev.* B **40** 2610
Yoshioka D 1989 *J. Phys. Soc. Japan* **58** 1516
Kane C L, Lee P A, Ng T K, Chakraborty B and Read N 1990 *Phys. Rev.* B **41** 2653

[8] Inui M, Doniach S and Gabay M 1988 *Phys. Rev.* B **38** 6631

[9] Chandra P, Coleman P and Larkin A I 1990 *J. Phys.: Condens. Matter* **2** 7933

[10] Emery V J, Kivelson S A and Lin H Q 1990 *Phys. Rev. Lett.* **64** 475
Marder M, Papanicolaou N and Psaltakis G C 1990 *Phys. Rev.* B **41** 6920

[11] Arovas D P and Auerbach A 1988 *Phys. Rev.* B **38** 316
Yoshioka D 1989 *J. Phys. Soc. Japan* **58** 32

[12] Chubukov A V 1984 *J. Phys. C: Solid State Phys.* **17** L991
Rastelli E, Reatto L and Tassi A 1985 *J. Phys. C: Solid State Phys.* **18** 353

[13] Forster D 1975 *Hydrodynamic Fluctuations, Broken Symmetry, and Correlation Function* (New York: Benjamin)

[14] Wagner H 1966 *Z. Phys.* **195** 273

[15] Pines D and Nozières P 1989 *The Theory of Quantum Liquids* vol 1 (London: Addison-Wesley)

[16] Ramakrishnan T V 1990 *Physica* B **163** 34